

# Optimally-Discriminative Voxel-Based Morphometry significantly increases the ability to detect group differences in Schizophrenia, Mild Cognitive Impairment, and Alzheimer's Disease

Tianhao Zhang<sup>1</sup> and Christos Davatzikos<sup>1</sup>

<sup>1</sup>Department of Radiology, University of Pennsylvania, Philadelphia, PA, United States

## Purpose

Voxel-Based Morphometry (VBM) has been widely applied for characterizing brain changes on structural Magnetic Resonance Imaging. However in the conventional VBM methods, Gaussian smoothing, which is always used prior to General Linear Model (GLM) [1] to integrate imaging signals from a region, proves critical due to lack of the spatial adaptivity necessary to optimally match image filtering with an underlying (unknown *a priori*) region of interest. In this work, Optimally-Discriminative Voxel-Based Analysis (ODVBA) [2], as a recently-developed method utilizing a new spatially adaptive smoothing scheme to determine group differences, is evaluated in comparison with the conventional VBM method, two other spatially adaptive smoothing methods, and two cluster enhancing methods, in three different studies on schizophrenia, mild cognitive impairment, and Alzheimer's disease.

## Method

The data collected for the three studies include [Dataset1](#) [3]: 69 schizophrenic patients and 79 controls; [Dataset2](#) [4]: 15 subjects with mild cognitive impairment (MCI) and 15 controls. [Dataset3](#) [5]: 50 MCI subjects had undergone conversion to AD and 50 MCI non-converters. A standard image pre-processing protocol [2] was used to generate the gray matter RAVENS map, which reflects the tissue density. Then, we implement six different methods of analysis including 1) ODVBA: it starts from a regional discriminative analysis, with non-negativity constraints, on a spatial neighborhood around each voxel to determine the optimal coefficients that best highlight the difference between two groups in that neighborhood. And then the weights determined for a given voxel from all the regional analyses it belongs to are combined into a map representing statistically significant voxel-wise group differences, using permutation tests; 2) the conventional VBM method: Gaussian smoothing with 8mm FWHM plus GLM (abbr. [GLM](#)); other two spatially adaptive smoothing methods: 3) Propagation-Separation ([PS](#)) [6] and 4) wavelet denosing ([WL](#)) [7], both of which are followed by GLM without Gaussian smoothing; and two versions of Threshold-Free Cluster Enhancement (TFCE) [8]: 5) the original GLM-based TFCE ([G-TFCE](#)) [8] in which 4mm FWHM is used as suggested, and 6) an ODVBA-based TFCE ([O-TFCE](#)) in which the TFCE scores are calculated based on the statistical images of ODVBA. FDR is employed to correct for multiple comparisons for all above methods.

## Results

For all six methods, the resulting  $p$  value maps are threshold by FDR corrected  $p=0.01$  in Dataset1 and FDR corrected  $p=0.05$  in Dataset2 and Dataset3. Note that GLM, PS, and WL did not produce significant results after FDR correction in Dataset 2. We focus on the comparisons in three criteria. 1) Spatial extent of the group difference: We display the total number of detected significant voxels obtained from all methods for three different datasets in Fig. 1. It is concluded that ODVBA is more sensitive than GLM since it detects more significant voxels. PS and WL produced smaller significant areas than either GLM or ODVBA. The two cluster enhancing methods, G-TFCE and O-TFCE, produced larger significant areas than the voxel-based statistical methods, and O-TFCE shows stronger statistical power than G-TFCE. For visual inspection, we demonstrate the surface renderings of detected regions in Fig. 2 (For limitation of space, only those of ODVBA and GLM are provided). 2) Significance of the group difference: On each anatomical region (prior defined), we calculated the  $t$  statistic based on means of RAVENS values of the detected area per region. We demonstrate the average  $t$  values of anatomical regions in Fig. 3. It is clear that ODVBA offers the highest  $t$  values whereas GLM produces the lowest values.  $t$  values of G-TFCE are generally lower than O-TFCE, further suggesting that Gaussian smoothing is inferior to our proposed spatially adaptive method. 3) Spatial agreement between detected regions and underlying tissue boundaries: In Fig. 4 we show the detected area of a small section near the hippocampus. We see that GLM blurs volumetric measurements from the hippocampus with such measurements from the fusiform. However, ODVBA delineates a more precise area of significant atrophy, which agrees with GM boundaries. Although PS and WL are capable of detecting tissue boundaries, this detection is weak. We can also see the G-TFCE and O-TFCE do not blur volumetric measurements as in GLM.

## Conclusions

In summary, ODVBA demonstrated highest significance in group differences within the identified voxels. In terms of spatial extent of detected area and agreement of anatomical boundary, it performed better than other tested voxel-based methods and competitively with both cluster-based methods. It is worth noting that for all tested criteria, O-TFCE performed better than the original G-TFCE, thereby indicating the synergistic value between ODVBA and TFCE.

## References

- [1] Friston et al., 1994, Statistical parametric maps in functional imaging: a general linear approach. *Hum. Brain Mapp.* 2, 189–210. [2] Zhang and Davatzikos, 2011, ODVBA: Optimally-Discriminative Voxel-Based Analysis. *IEEE Trans. Medical Imag.* 30, 1441-1454. [3] Davatzikos et al., 2005. Whole-brain morphometric study of schizophrenia revealing a spatially complex set of focal abnormalities. *Arch. Gen. Psychiatry* 62, 1218–1227. [4] Davatzikos et al., 2008, Detection of prodromal Alzheimer's disease via pattern classification of magnetic resonance imaging. *Neurobiol. Aging* 29, 514–523. [5] Misra et al., 2009, Baseline and longitudinal patterns of brain atrophy in MCI patients, and their use in prediction of short-term conversion to AD: results from ADNI. *NeuroImage* 44, 1415–1422. [6] Polzehl and Spokoiny, 2000, Adaptive weights smoothing with applications to image restoration. *J. R. Statist. Soc. B* 62, 335–354. [7] Pizurica et al., 2003, A versatile wavelet domain noise filtration technique for medical imaging. *IEEE Trans. Medical Imag.* 22, 323–331. [8] Smith and Nichols, 2009, Threshold-free cluster enhancement: Addressing problems of smoothing, threshold dependence and localisation in cluster inference, *NeuroImage* 44, 83-98.

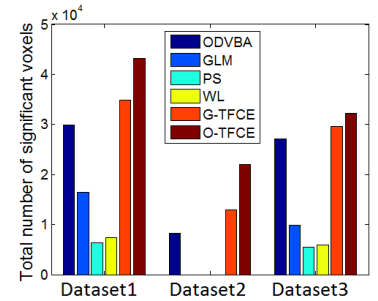


Figure 1: The total number of significant voxels of different methods.

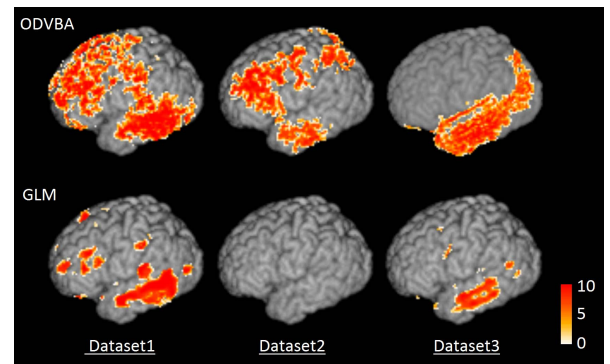


Figure 2: Surface renderings of regions detected in the three datasets. Color bar indicates  $-\log(p)$  value.

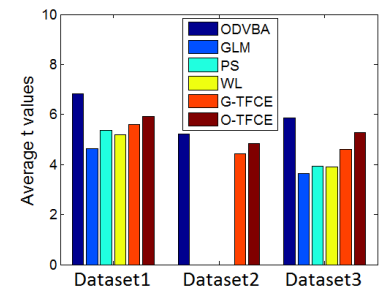


Figure 3: The average  $t$  values of anatomical regions of different methods.

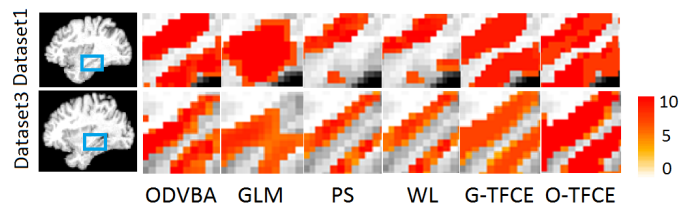


Figure 4: Results in the local area near the hippocampus. Two representative sections are selected from two analyses. Color bar indicates  $-\log(p)$  value.